

# Minimal Multifractality in the Spectrum of a Quasiperiodic Hamiltonian

Gerardo G. Naumis

*Instituto de Física, Universidad Nacional Autónoma de México (UNAM),  
Apartado Postal 20-364, 01000, México, Distrito Federal, Mexico.*

(Dated: October 17, 2018)

In many systems, the electronic energy spectrum is a continuous or singular continuous multifractal set with a distribution of scaling exponents. Here, we show that for a quasiperiodic potential, the multifractal energy spectrum can have a minimal dispersion of the scaling exponents. This is made by tuning the ratio between self-energies in a tight-binding Hamiltonian defined in a quasiperiodic Fibonacci chain. The tuning is calculated numerically from a trace map, and coincides with the place where the scaling exponents of the map, obtained from cycles with period six and two, are equal. The diffusion of electronic wave packets also reflects the minimal multifractal nature of the spectrum, by reducing intermittency. The present result can help to simplify the task of studying several problems in quasiperiodic systems, since the effects of multiscaling are better isolated.

PACS numbers:

Quasiperiodic systems, which are neither periodic, nor disordered, have been the focus of an active research since the seventies [1, 2]. Later on, they gained much more importance when the discovery of alloys with five-fold symmetry and long range order was made [3]. These alloys were called quasicrystals, in recognition of their quasiperiodic atomic structure. The word quasiperiodic means that the structure can be represented as a sum of periodic functions, each with an incommensurate period with respect to the others. Still, the nature of the physical properties of quasicrystals is not well understood [4][5][6]. Even in the theoretical side there is a lack of understanding in how electrons propagate, specially in two and three dimensions [7]. As is well known, a periodic potential satisfies the Bloch's theorem, which tells that the eigenstates of the Schrödinger equation are plane waves of delocalized nature, and the energy spectrum is continuous [8]. For disordered systems, like in the one dimensional (1D) Anderson model, all the states are localized corresponding to isolated eigenvalues [9]. In more dimensions, there is a mobility edge which separates extended from localized states [9]. For most of the quasiperiodic systems in 1D, the spectrum is neither continuous nor singular, instead a new type of spectrum, called singular continuous is obtained [10]. This kind of spectrum is similar to a Cantor set, and presents a multifractal nature. The corresponding eigenfunctions are called critical, and also show self-similarity and multifractality. In two and three dimensions, the nature of the spectrum is not known, although there seems to be a kind of mobility edge [11][12]. However, even in 1D, where large amount of work has been done, there are many unsolved questions, like the nature of conductivity [14] or diffusivity [15], the spectral statistics and the shape of many of the eigenfunctions [16][17]. For example, Machida *et. al.* [18] showed that for certain parameters of the quasiperiodic Harper equation, the distribution of level spacing follows an inverse power law. This tendency was explained by Geisel *et. al.* [19] as a level clustering. More recently [20], it has been argued that the clustering

regimen of the distribution of level spacings in quasiperiodic potentials was an artifact of an inappropriate way of making the unfolding procedure, and the fact that the distribution of gaps and bands were different was considered as a signature of different scaling indices in the spectrum [20].

Many of the difficulties that arise in the studies of quasiperiodicity, are due to the fact that all of the systems that have been used up to now, present a multifractal spectrum [15][19][20][21], *i.e.*, the scaling with the system size is not given by only one scaling exponent ( $\alpha$ ), instead a distribution of exponents determined by a function called  $f(\alpha)$  is usually found. This makes very difficult to relate the spectrum with the corresponding eigenfunctions, since they have a complicate shape due to *multiscaling* and *intermittency*. For example, the moments of a wave packet that is diffusing behave as  $\langle x^q(t) \rangle \sim t^{q\beta(q)}$  for a time  $t$ , where  $\beta(q)$  is an exponent related with the spectral type. In principle, it seems that one needs to exclude any simple relation between spectral and diffusion exponents [15][22]. However, as we show in this letter, the problem can be more transparent if the parameters of the quasiperiodic potential are chosen in such a way that the system presents a minimal dispersion of scaling exponents. As a consequence, instead of dealing with a wide multifractal set, which makes all computations very demanding from a technical point of view, one considers a very narrow multifractal set, which is much closer to a pure monofractal. Thus, it is possible to improve the isolation of *intermittency*, without dealing with huge *multiscaling*.

As starting point, we use the simplest model of a quasicrystal: the Fibonacci chain (FC). The FC is build as follows: consider two letters,  $A$  and  $B$ , and the substitution rules,  $A \rightarrow B$ , and  $B \rightarrow AB$ . If one defines the first generation sequence as  $\mathcal{F}_1 = A$  and the second one as  $\mathcal{F}_2 = BA$ , the subsequent chains are generated using the two previous rules, for instance,  $\mathcal{F}_3 = ABA$ . Starting with an  $A$ , we construct the following sequences,  $A$ ,  $B, AB$ ,  $BAB$ ,  $ABBAB$ ,  $BABABBAB$ , and so on. Each

generation obtained by iteration of the rules is labeled with an index  $l$ . Is clear that the number of letters in each generation  $l$  is given by the Fibonacci numbers  $F(l)$  of generation  $l$ , which satisfy:  $F(l) = F(l-1) + F(l-2)$  with the initial conditions:  $F(0) = 1, F(1) = 1$ . A natural model for a one dimensional quasicrystal is a tight-binding hamiltonian of the type,

$$E\psi_n = V(n)\psi_n + t_n\psi_{n+1} + t_{n-1}\psi_{n-1} \quad (1)$$

where  $\psi_n$  is the wave-function at site  $n$ ,  $t_n$  is the resonance integral between sites  $n$  and  $n+1$ .  $V(n)$  is the atomic on-site potential and  $E$  are the allowed energies. For the present purposes,  $t_n$  is set to 1 for all sites, and  $V(n)$  has two possible values,  $V_A$  and  $V_B$  following the Fibonacci sequence. In fact, using a Fourier expansion, we can show that the Fibonacci potential is no more than a sum of well known Harper potentials,

$$V(n) = \bar{V} + 2\delta V \sum_{s=1}^{\infty} \tilde{V}(s) \cos(\pi s \phi(2n+1)) \quad (2)$$

where  $\phi$  is the golden mean  $\phi = (\sqrt{5}+1)/2$ ,  $\bar{V} = (V_A/\phi) + (V_A/\phi^2)$ , and  $\tilde{V}(s)$  is the  $s$  harmonic of the Fourier series,  $\tilde{V}(s) = \sin(\pi s \phi)/s\phi$ . The strength of the quasiperiodicity is measured by the difference between site-energies  $\delta V = V_A - V_B$ .

The spectrum of this problem, *i.e.*, the energies that satisfy eq.(1), are obtained by using the trace of the transfer matrices. These energies are those for which the trace of generation  $l$  (that we denote by  $2x_l(E)$ ) of the transfer matrix satisfy  $-1 \leq x_l(E) \leq 1$ . In the case of a FC,  $x_l(E)$  can be obtained from a non-linear map given by [23],

$$x_{l+1}(E) = 2x_l(E)x_{l-1}(E) - x_{l-2}(E), \quad (3)$$

with the initial conditions  $x_{-1} = 1, x_0 = (E + \lambda)/2, x_1 = (E - \lambda)/2$ , and  $\lambda = |\delta V|/2$ . Since the map contains three successive generations, one can consider the evolution of the trace as a trajectory in a 3D space. It has also been shown that the spectrum is a multifractal set [24], and it was conjectured that the exponents describing the scaling of the spectrum near the upper band edge and band center were governed by cycles of periods 6 and 2 of the trace map. Using a linearized stability analysis around these cycles, two scaling indices were found [25], one corresponding to the period 6 cycle,

$$\alpha_6 = \frac{\ln \left\{ [1 + 4(1 + \lambda^2)^2]^{1/2} + 2(1 + \lambda^2) \right\}^2}{\ln \phi^6}, \quad (4)$$

and the other to the period 2 cycle,

$$\alpha_2 = \frac{\ln \left\{ 8J - 1 + [(8J - 1)^2 - 4]^{1/2} \right\} / 2}{\ln \phi^2} \quad (5)$$

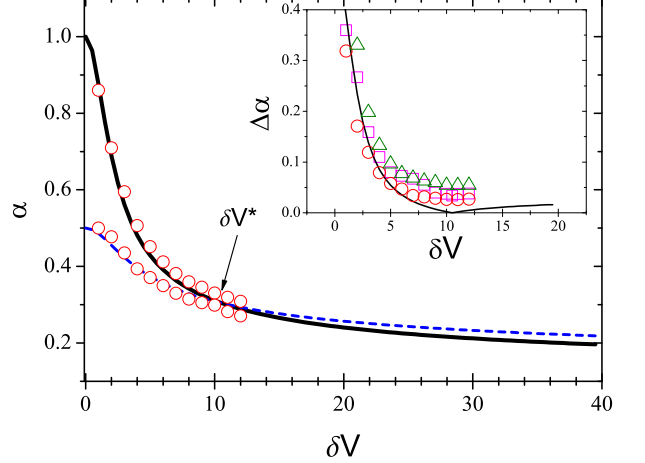


FIG. 1: Scaling exponents  $\alpha_6$  (solid line) and  $\alpha_2$  (dotted line) as a function of  $\delta V$ . The arrow indicates the place where  $\alpha_6 = \alpha_2$ . The numerical results are shown as circles. Inset: absolute value of the difference between  $\alpha_{\max} - \alpha_{\min}$  for different values of  $\delta V$ . The triangles, squares and circles are the numerical results for generations  $l = 9, 12$  and  $15$  respectively. The solid line is the absolute value of the difference between  $\alpha_6$  and  $\alpha_2$ .

with  $J = [3 + (25 + 16\lambda^2)^{1/2}]/8$ . In Ref. [24], it was concluded that  $\alpha_2$  was the minimum scaling exponent, related with the band-width of the upper band edges,  $\alpha_6$  was the maximal scaling exponent. Between them, a continuous distribution of exponents was found. That argument can be related with the shape of the wave-function, and in principle it is possible to conclude that wave-functions in the edges decay more rapidly than in the center of the spectrum [24]. Later on, it was proved that the 6 cycle does not always occur at the center or edges of the spectrum, and in fact, the question of which is the maximal contraction factor is an open question, since there are other cycles [26]. In spite of this, in fig. 1 we show a plot of scaling exponents from cycles 6 and 2, where is clearly seen that not always  $\alpha_2 < \alpha_6$ , as was erroneously stated in ref. [24].

Furthermore, there is a cross-over of the two scaling exponents. The exponent  $\alpha_2$  is the minimum only from  $\delta V = 0$  to  $\delta V \approx 10.5$ . The crossover occurs when  $\alpha_2 = \alpha_6$ . The special value of  $\delta V^*$  where this happens can be calculated by making Eq. (4) equal to Eq. (5). After many lengthy algebraic steps, it is possible to show that  $\delta V^*$  is given by the irrational number,

$$\delta V^* = 2\sqrt{13 + \frac{11}{2}\sqrt{7}} \approx 10.497929740830855719340651...$$

This value perfectly agrees with the plot of  $\alpha_6$  and  $\alpha_2$ . In the special value  $\delta V^*$ ,  $\alpha_6 = \alpha_2 = d_f^* \approx 0.305$ . If as stated in ref. [24], the 6 and 2 cycles were the extremal scaling exponents, then  $\alpha_{\max} = \alpha_{\min}$  at  $\delta V^*$ , and

thus one should expect only one scaling exponent, corresponding to a pure monofractal. To test how far is this assumption from the real behavior of the spectrum, we have performed numerical calculations. First, the band widths of the spectrum were obtained by the iteration of the map (3), using quadruple precision (32 significant digits) for each value of  $\delta V$ . The calculations were made for chains of generations  $l = 9, 12$  and  $15$ . The maximal and minimal scaling exponents have the following expression,

$$\alpha_{\max} = \frac{\ln \Delta E_0 - \ln F(l)}{\ln \Delta E_{\min}(l)}, \alpha_{\min} = \frac{\ln \Delta E_0 - \ln F(l)}{\ln \Delta E_{\max}(l)} \quad (6)$$

where  $\Delta E_0$  is the initial band width, and  $\Delta E_{\min}(l)$  ( $\Delta E_{\max}(l)$ ) are the minimal (maximal) bandwidths of a  $l$  generation FC. The contribution of  $\Delta E_0$  tends to zero in an infinite system, but is needed in the present finite case. Figure 1 shows the numerical values of  $\alpha_{\max}$  and  $\alpha_{\min}$  for  $l = 15$  compared with the theoretical values. In spite that  $\alpha_6$  and  $\alpha_2$  are not the maximal and minimal scaling exponents, they are close to the numerical values, and a minimal dispersion of the spectrum is seen at  $\delta V^*$ . The reason of the very close values of the real extremal exponents,  $\alpha_{\max}$  and  $\alpha_{\min}$ , compared with  $\alpha_6$  and  $\alpha_2$ , is because these cycles dominates the spectrum when  $\delta V \rightarrow \infty$ . Notice that beyond  $\delta V = 12$ , there are no numerical points due to the increased difficulty in computing the band widths, since a lot of precision is required as  $\delta V \rightarrow \infty$ .

It is also possible to calculate the multifractal distribution  $f(\alpha)$  of scaling exponents. Let us denote the bandwidth of the  $i$ -th band of the spectrum by  $\Delta E_i$ . Each band contains the same measure or density of states  $1/F(l)$ . Each band scales as:  $(\Delta E_i)^\alpha = 1/F(l)$ . A partition function is defined by [27],

$$\Gamma_l(q, \tau) = \sum_{i=1}^{F(l)} \left( \frac{1}{F(l)} \right)^q \left( \frac{1}{\Delta E_i} \right)^\tau \quad (7)$$

This function has a limit when  $l$  goes to infinity, which is either zero or infinity, unless  $\tau$  and  $q$  are chosen in an appropriate way [27] such that  $\Gamma_l(q, \tau) = 1$ . This condition determines a function  $\tau(q)$ . The fractal dimension for a set of points with the scaling  $\alpha$ , is obtained by a Legendre transformation  $f(\alpha) = -\tau(q) + \alpha q$ , where  $\alpha = d\tau(q)/dq$ . In figure 2, the evolution of  $f(\alpha)$  versus  $\alpha$  is shown for different values of  $\delta V$  using generation  $l = 9$ . Notice how the width of the curves decrease and in fact is a minimum as  $\delta V \rightarrow \delta V^*$ . The width of the curve  $f(\alpha) = 0$  also defines the values of  $\alpha_{\min}$  and  $\alpha_{\max}$ . This can also be seen in the inset of fig. 1, where we plot the absolute value of the difference  $\Delta\alpha = |\alpha_{\max} - \alpha_{\min}|$  for different generations. Observe that  $f(\alpha)$  has a finite width at  $\delta V^*$ , and thus  $\alpha_{\min} \neq \alpha_{\max}$ . This rules out the possibility of having a pure monofractal spectrum, which was something to be desired. However, the numerical calculations suggests that  $\delta V^*$  is the value where the spectrum has a minimal multifractal dispersion.

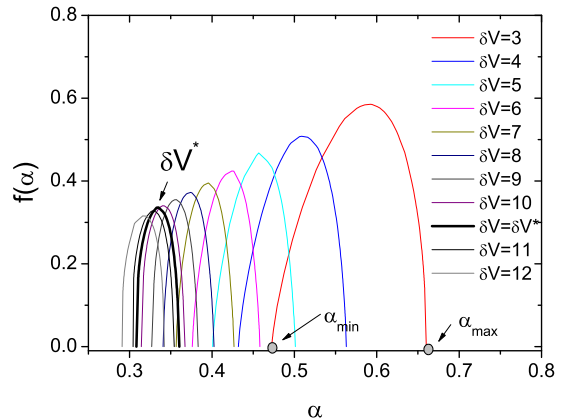


FIG. 2: Evolution of  $f(\alpha)$  as  $\delta V$  is changed for a FC of generation  $l = 9$ . From right to left,  $\delta V = 3, 4, 5, 6, 7, 8, 9, \delta V^*, 11, 12$ . The special value  $\delta V^*$  is indicated with an arrow. As an example,  $\alpha_{\max}$  and  $\alpha_{\min}$  are indicated for  $\delta V = 3$ .

Since there is a close relationship between band scaling, localization and the dispersion of electronic wave functions [28], one can expect to observe the signature of minimal multifractality in the electron diffusion. A way of characterizing the propagation consists in the study of the wavefunction moments as a function of time [15], which are defined as,

$$\langle x^q(t) \rangle = \sum_{n=1}^{F(l)} (n - n_0)^q \Psi^*(n, t) \Psi(n, t)$$

where  $j$  is the site position in the chain.  $\Psi(n, t)$  is the wavefunction at time  $t$  on site  $n$ , that evolves following the time dependent Schrödinger equation, in which  $E$  is replaced by the operator  $-i\partial/\partial t$ . As was already stated, in quasiperiodic systems  $\langle x^q(t) \rangle$  follows a power law behavior of the type  $\langle x^q(t) \rangle = \mathcal{D}(q)t^{q\beta(q)}$ , where  $\mathcal{D}(q)$  is a constant, known as the diffusion constant for the periodic case. In the present work, we have performed numerical simulations to obtain  $\beta(q)$  by using chains of generation  $l = 15$ . As initial conditions, a delta function wave-packet is dropped at time  $t = 0$  at site  $n_0$ . Different initial sites were used, but the results are almost  $n_0$  independent. The numerical computations were made by solving the time dependent Schrödinger equation by two methods that gave similar results. The first was a direct numerical resolution of the differential Schrödinger equation using a discretization of time, and the second consists in a decomposition in eigenfunctions. Since each eigenfunction evolves independently with time, the resulting wave function at any time is just a linear combination of eigenfunctions, where the coefficients of the combination are the projections of the initial condition into each eigenvector. For long times, the second method is much more accurate. Finally, the scaling exponents

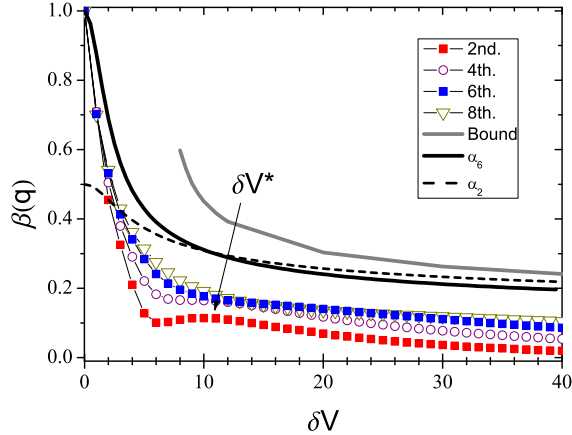


FIG. 3:  $\beta(q)$  as a function of the difference in self-energies  $\delta V$  for  $q = 2, 4, 6$  and  $8$ . A rigorous bound for  $\beta(q)$  is shown with a grey line. Also, the scaling exponents  $\alpha_6$  and  $\alpha_2$  are shown with solid and dotted lines respectively.

$\beta(q)$  were obtained by fitting a power law in a log-log plot of  $\langle x^q(t) \rangle$  versus  $t$ . In all of the cases, the fit was made from  $t = 1000$  to  $t = 50000$  (all units have been set to one) in order to avoid initial transients.

Figure 3 shows the values of  $\beta(q)$  as a function of  $\delta V$  for the first eight moments. Observe that odd moments are not displayed since they are zero. The graph shows a very interesting feature which is a nearly collapse of  $\beta(q)$  for  $q = 4, 6$  and  $8$  at  $\delta V^*$ . This suggests that  $\beta(q) \rightarrow \beta^* \approx 0.16$  for such values of  $q$ . A local maximum is obtained

for  $q = 2$ . Since  $\beta^*$  is nearly  $q$  independent, and  $\beta(q)$  is different from one, is clear that the wave functions show intermittency but almost no multiscaling, although this effect is mitigated since  $\beta(2)$  has a lower value. In figure 3 we have also included the values of  $\alpha_{\min}$  and  $\alpha_{\max}$  as a comparison. Notice the crossover near the collapse of  $\beta(q)$ . The fact that  $\beta(q)$  and  $\alpha$  are represented in the same graph is not just a coincidence, since the scaling of the spectrum is related with wave-localization. In fact, the present work suggests that in a very rough approximation  $d_f^* \approx \beta^*/2$ , which is similar to the result obtained from a analysis of the relationship between wave localization overlap and the spectrum [29]. Also, in figure 3 we present a comparison with a strict mathematical bound that has recently been proved [30] for  $\beta(q)$  when  $\delta V > 8.0$ . The bound works as predicted, although is higher than the actual values of  $\beta(q)$ .

In conclusion, we have shown a value of the Fibonacci potential for which there is a minimal dispersion in the scaling exponents of the multifractal spectrum. The value of the potential seems to be determined mainly by the six and two cycles. The behavior of wave packet diffusion reflects this fact by showing almost no multiscaling. We hope that the present work will bring much more understanding into the properties of quasiperiodic Hamiltonians, since one can better isolate effects of multiscaling. For example, it would be useful to study the evolution of the spectral statistics near this minimal condition. Since the trace map is similar for phonons or the case of quasiperiodic hopping integrals, the presented property can be extended to such cases, or different trace maps [31].

I would like to thank DGAPA-UNAM project IN-117806 for financial help.

- 
- [1] D.R. Hofstadter, Phys. Rev. B **14** (1976) 2239.
  - [2] S. Aubry, G. Andre, in: Colloquium on Group Theoretical Methods In Physics, Preprint, (1979). Reprinted in: *The physics of quasicrystals*, ed. by P. Steinhardt and Stellan Ostlund, (World Scientific, Singapore, 1987).
  - [3] D. Shechtman, I. Blech, D. Gratias, J.W. Cahn, Phys. Rev. Lett. **53**, 1951 (1984).
  - [4] P. Thiel, and J.M. Dubois, Nature **406**, 571(2000).
  - [5] E.Y. Vedmendenko, U. Grimm, R. Wiesendanger, Phys. Rev. Lett. **93**, 076407, (2004).
  - [6] P. Moras, et. al., Phys. Rev. Lett. **96**, 156401 (2006).
  - [7] E. Macia, Rep. Prog. Phys. **69**, 397 (2006).
  - [8] Ch. Kittel, Introduction to Solid-State Physics, 7th. ed., Wiley, New York, (1996).
  - [9] Zallen, The physics of amorphous solids, J. Wiley & Sons, New York (1983).
  - [10] A. Sütő, in *Beyond Quasicrystals*, ed. by F. Axel and D. Gratias, Les Editions de Physique, France, (1994).
  - [11] G.G. Naumis, R.A. Barrio, Ch. Wang, Phys. Rev. B **50**, 9834 (1994).
  - [12] G.G. Naumis, J. Phys.: Condens. Matter **11**, 7143 (1999).
  - [13] P. Tong, B. Li, B. Hu, Phys. Rev. Lett. **88**, 046804 (2002).
  - [14] E. Maciá, F. Domínguez-Adame, Phys. Rev. Lett. **79**, 5301 (1991).
  - [15] R. Ketzmerick, K. Kruse, S. Kraut, T. Geisel, Phys. Rev. Lett. **79**, 1959 (1997).
  - [16] T. Fujiwara, M. Kohmoto, T. Tokihiro, Phys. Rev. B **40**, 7413 (1989).
  - [17] E. Macia, Phys. Rev. B **60**, 10 032 (1999).
  - [18] K. Machida, M. Fujita, Phys. Rev. B **34**, 7367 (1986).
  - [19] T. Geisel, R. Ketzmerick, G. Petschel, Phys. Rev. Lett. **66**, 1651 (1991).
  - [20] S.N. Evangelou, J.L. Pichard, Phys. Rev. Lett. **84**, 1643 (2000).
  - [21] Ch. Tang, M. Kohmoto, Phys. Rev. B **34**, 2041 (1986).
  - [22] F. Piéchon, Phys. Rev. Lett. **76**, 4372 (1996).
  - [23] M. Kohmoto, L.P. Kadanoff, C. Tang, Phys. Rev. Lett. **50**, 1870 (1983).
  - [24] M. Kohmoto, B. Sutherland, Ch. Tang, Phys. Rev. B **35**, 1020 (1987).

- [25] M. Kohmoto, Y. Oono, Phys. Lett. A **102**, 145 (1984).
- [26] A. Rüdinger, F. Piéchon, J. Math. Phys. A: Math. Gen. **31**, 155 (1998).
- [27] T.C. Halsey, M.H. Jensen, L.P. Kadanoff, I. Procaccia, B.I. Sharaiman, Phys. Rev. A **33**, 1141 (1986).
- [28] G.G. Naumis, *Phys. Rev. B* **59**, 11315 (1999).
- [29] G.G. Naumis, J. of Phys.: Cond. Matter. **15**, 5969 (2003).
- [30] D. Damanik, S. Tcheremchantsev to be published.
- [31] X. Wong, U. Grimm, M. Schriber, Phys. Rev. B **62**, 14020 (2000).